Anal Bioanal Chem (2009) 393:1943–1948
DOI 10.1007/s00216-009-2687-y

ORIGINAL PAPER

Aptamer-based electrochemical biosensor for *Botulinum* neurotoxin

Fang Wei · Chih-Ming Ho

Received: 12 December 2008 / Revised: 28 January 2009 / Accepted: 4 February 2009 / Published online: 24 February 2009

Abstract We have developed an aptamer-based electrochemical sensor for detection of *Botulinum* neurotoxin, where steric hindrance is applied to achieve specific signal amplification via conformational change of the aptamer. The incubation time and potassium concentration of the reaction buffer were found to be key parameters affecting the sensitivity of detection of the recognition of *Botulinum* neurotoxin by the aptamer. Under optimized experimental conditions, a high signal-to-noise ratio was obtained within 24 h with a limit of detection (LOD) of 40 pg/ml by two standard deviation cutoffs above the noise level.

Keywords Aptamer · *Botulinum* neurotoxin · Biosafety · Electrochemical biosensors · Steric hindrance · Conducting polymer · Bioanalytical methods · Bioassays · Biosensors

Introduction

Botulinum neurotoxin (*Bo*NT) is among the most toxic substances known [1, 2]. Modeling studies shows 4 g per gallon of *Bo*NT in milk could cause rapid distribution more than 400,000 causalities within days [3]. Therefore, rapid and sensitive detection of *Bo*NT are highly desirable for addressing biosafety concerns. Among the seven defined serotypes of *Bo*NT (A to G), type A is the most frequent cause of cases of human botulism [4]. Conventional methods for detection of *Bo*NT are primarily immunoassay-based and have a sensitivity of 2–60 pg/ml [5, 6]. However, immunoassay of *Bo*NT requires time-consuming and labor-intensive process of screening highly specific human monoclonal antibodies [5, 7]. In contrast, aptamers are fragments of oligonucleotides which can bind specifically to target proteins in the presence of appropriate conformational change [8–10] and have the advantages of simpler screening methods, higher stability than antibodies and reusability. Recently, an efficient single micro-bead SELEX approach has been developed to generate high-affinity single-stranded DNA (ssDNA) aptamers against aldehyde-inactivated *Botulinum* neurotoxin type A (*Bo*NT/A) [11]. The individual dissociation constants (K_ds) range from 3 nM to 50 nM for different aptamer designs.

Here, we propose a strategy that combines an electrochemical method [12–15] with enzymatic amplification and an aptamer probe that undergoes target-induced conformational change for the detection of *Bo*NT/A toxoid (*Bo*NT/A). The electrochemical sensor has a streptavidin-dendrimer-interfaced polypyrrole substrate to maintain the activity of the aptamer and *Bo*NT/A. The aptamer is dual-labeled with a reporting tag (fluorescein) and an anchoring tag (biotin). In the signal amplification process, an anti-fluorescein antibody conjugated to horseradish peroxidase (HRP) is introduced to bind to the fluorescein label on the aptamer. After antibody binding 3, 3′, 5, 5′ tetramethylbenzidine (TMB/H_2O_2) is added for the signal readout under −200 mV potential. TMB acts as a mediator and is reduced at −200 mV; the reduced TMB reduces the oxidized form of HRP. HRP then reduces H_2O_2 to $2H_2O$ and the HRP is oxidized. This signal amplification process only occurs

F. Wei · C.-M. Ho (✉)
Department of Mechanical and Aerospace Engineering,
School of Engineering and Applied Science,
University of California at Los Angeles,
420 Westwood Plaza,
Los Angeles, CA 90095-1597, USA
e-mail: chihming@ucla.edu

under conditions that permit HRP binding to the aptamer on the surface. In the absence of *Bo*NT/A binding, the aptamer remains in the closed state and steric hindrance [16, 17] from the sensor surface inhibits signal amplification by preventing anti-fluorescein-HRP from accessing the reporting tag fluorescein. After binding to *Bo*NT/A, the aptamer conformation opens up and permits access of the HRP reporter, generating an electrochemical current signal. Therefore, only the specific target *Bo*NT/A can generate an amplified current.

Materials and methods

Aptamer and *Bo*NT/A toxoid

HPLC-purified aptamer oligonucleotides, biotin-labeled on the 5′ end and fluorescein-labeled on the 3′ end, were custom-synthesized (Operon Inc., Alabama, USA). Biotin bound to surface streptavidin served as an anchor to the electrode and the fluorescein label allowed for binding of anti-fluorescein-HRP to amplify the electrochemical current signal.

The 76-bp aptamer sequence for *Bo*NT/A detection [11] was 5′-ATACCAGCTTATTCAATT GAC ATG ACT GGG ATT TTT GGC GAA ATC GAA GGA AGC GGA GAGATAGTAAGTGCAATCT-3′.

Secondary structure and G-quadruplex searches were done using Mfold [18, 19] and QGRS Mapper [20]. Two possible G-quadruplex sequences were identified in the *Bo*NT/A aptamer, one beginning at position 28 with a length of 29 bp and the other beginning at position 29 with a length of 28 bp. Possible folding positions are underlined in the following sequences:

G-quadruplex 1: GGGATTTTTGGCGAAATCGAA GGAAGCGG
G-quadruplex 2: GGATTTTTGGCGAAATCGAA GGAAGCGG

*Bo*NT/A toxoid (toxin inactivated by formaldehyde treatment) with a molecular weight of 150 kDa was purchased from Metabiologics, Inc (Madison, WI).

Surface fabrication of streptavidin-polypyrrole electrodes

The electrode surface consisted of a conducting layer of streptavidin-coated polypyrrole (PPy) polymerized on gold thin film. Streptavidin was introduced into the PPy matrix by copolymerization of a streptavidin-modified DNA dendrimer (Genisphere, USA, diameter 70–90 nm) and pyrrole (Sigma, USA). The streptavidin-modified DNA dendrimer was composed of short oligonucleotides and could be easily incorporated into the PPy matrix due to the negative charge of the dendrimer. Each dendrimer was labeled with two to four streptavidin molecules.

For electropolymerization, the streptavidin-labeled dendrimer was diluted with pyrrole in 1× PBS (pH 7.5, Invitrogen, USA) at a ratio of 1:200 (*v*/*v*) for a final concentration of 10 mM pyrrole. The electrodes were covered with the mixture of dendrimer and pyrrole prior electropolymerization. To avoid exposure of the dendrimer to a strong electrical field and to form a smooth polymer surface, square-wave electrical field was applied for electropolymerization [21]. Each square-wave consisted of 9 s at a potential of +350 mV and 1 s at +950 mV. A total of 20 cycles of square-waves was applied and the entire process lasted for 200 s. After polymerization, the electrode was rinsed with ultra pure water (18.3 MΩcm) and dried under a stream of pure N_2. The polymer film was 51.5± 3.0 nm thick, as measured by a profilemeter (Dektak 6 Surface Profile Measuring System, Veeco). The surface concentration of streptavidin-modified dendrimer was 0.30± 0.05 pmol/cm^2, as measured with a scanning electron microscope (Hitachi S4700 SEM, Japan).

Electrochemical detection

The electrochemical sensor consisted of a 16-unit gold array. Each unit was comprised of three electrodes, including the working electrode (WE), counter electrode (CE), and reference electrode (RE) [17, 22]. The reference electrode was determined to be +218 mV vs. SCE by measuring cyclic voltammetric curves of 0.1 mM $[Fe(CN)_6]^{3-/4-}$. All electric potentials described in this report are in reference to the gold reference electrode (+218 mV vs. SCE) [17].

Two protocols were tested for aptamer-based *Bo*NT/A toxoid detection. One protocol was based on surface recognition and the other was based on recognition in bulk solution, followed by transfer onto the surface. For surface recognition, 100 nM (50 μl) aptamer, dual-labeled with biotin and fluorescein, in 1× Tris–HCl was first loaded onto the electrode for conjugation to the streptavidin dendrimer; the chip was washed and dried after 5 min of incubation. Different concentrations of *Bo*NT/A toxoid in volumes of 50 μl were then loaded onto the aptamer-coated surface. In the second protocol, mixtures of *Bo*NT/A toxoid at different concentrations and 100 nM aptamer (50 μl total) were first incubated for different periods of time and then transferred onto the electrodes. To optimize the binding efficiency, the effects of incubation times ranging from 1 h to 24 h were investigated. In both protocols, the recognition buffer was 1× Tris–HCl containing 15 mM KCl, 140 mM NaCl, 1 mM $MgCl_2$, and 1 mM $CaCl_2$. Since the efficiency of aptamer binding to *Bo*NT/A is correlated with metal cation concentration [23, 24], buffers with different concentrations

of KCl were also investigated. In both protocols, the electrical field was applied to achieve effective binding and correct folding of the aptamer [17, 25] with 20 cycles of 9 s at−300 mV and 1 s at +200 mV, followed by washing and drying. To generate amplification of signal specific for *Bo*NT/A, HRP conjugated to anti-fluorescein antibody (Roche, USA) in casein/PBS buffer (50 μl; Pierce, USA) was incubated with the electrodes for 5 min followed by washing and drying of the chip. Finally, amperometric measurements were carried out in the presence of 3, 3′, 5, 5′ tetramethylbenzidine (TMB/H_2O_2, Neogen Corp., Lexington, Kentucky, USA) low-activity substrate at −200 mV. In our experiments, the electrochemical signal was the current generated by the redox cycles between TMB, the HRP reporter enzyme, and H_2O_2. All experiments were performed at room temperature (Fig. 1).

Results

In-solution or surface-associated folding of the *Bo*NT/A aptamer

Detection of *Bo*NT is based on the signal generated by the conformational change of the aptamer. Correct folding of the aptamer allows high-affinity binding between the aptamer and *Bo*NT/A toxoid; misfolding and non-folding result in low signal-to-noise ratios (SNRs) [26]. In addition, the specific signal amplification is strongly dependent on the conformation of the aptamer before and after binding to *Bo*NT/A. Strong signal is generated by completely unfolded aptamer binding to target *Bo*NT/A and low noise occurs in the presence of fully folded aptamer in the absence of target. Therefore, understanding how to obtain correct folding of aptamer is key to the detection process.

Specificity of *Bo*NT/A aptamer binding was first investigated by comparing the signal obtained with different target proteins. Four non-target proteins were selected as controls: 1% BSA, 0.1% casein, 100 ng/ml IL-8, and 100 ng/ml IL-1b and *Bo*NT/A was assayed at a concentration of 100 ng/ml. *Bo*NT/A aptamer alone was included as a control. Figure 2 shows that the strongest signal was generated by *Bo*NT/A aptamer binding to *Bo*NT/A. This observation supports the assumption that the aptamer maintains a closed conformation in the presence of nonspecific target proteins and unfolds in the presence of the complementary target. It also indicates the high specificity of aptamer binding to *Bo*NT/A toxoid.

Aptamer-based detection of *Bo*NT/A can occur either on the surface or in solution. In both processes, three factors

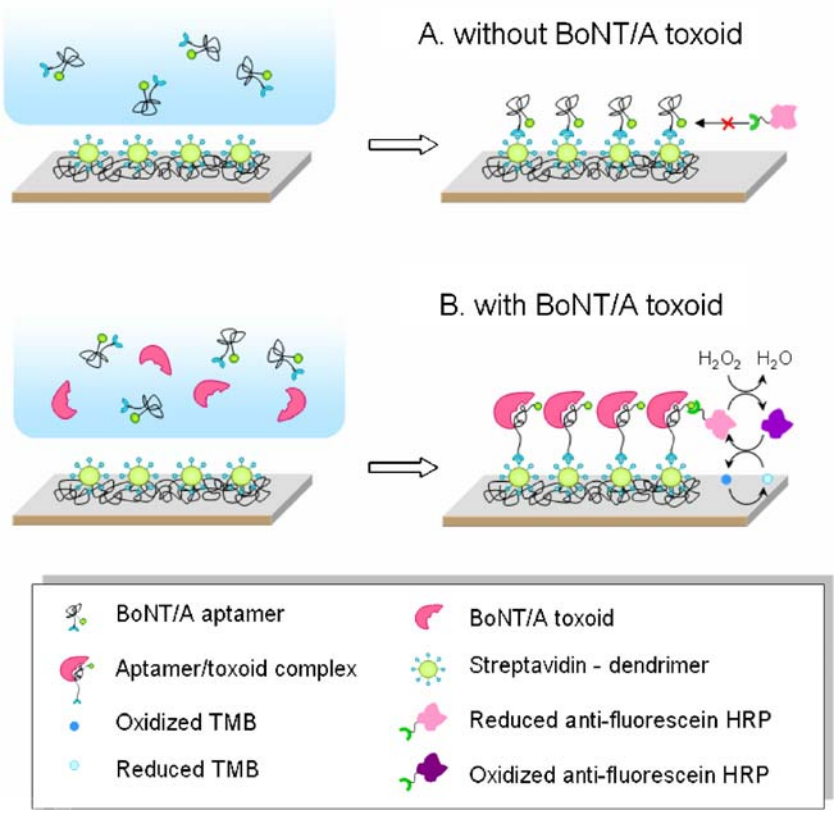

Fig. 1 Aptamer-based electrochemical detection of *Bo*NT/A toxoid

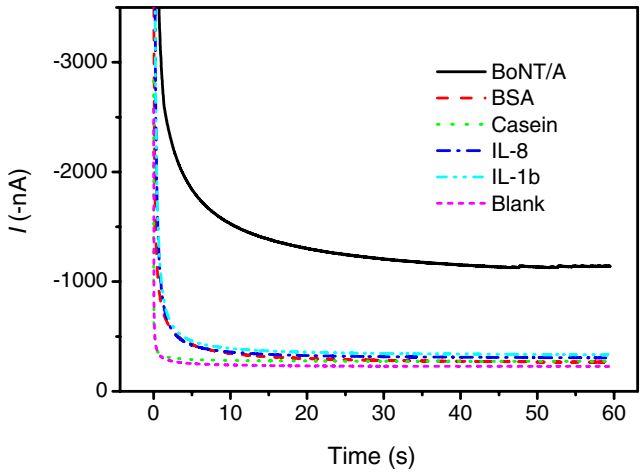

Fig. 2 Specificity of aptamer binding to *Bo*NT/A toxoid. *Bo*NT/A aptamer was incubated with 100 ng/ml *Bo*NT/A toxoid, 1% BSA, 0.1% Casein, 100 ng/ml IL-8, 100 ng/ml IL-1b, or PBS alone (blank)

affect the final readout: the efficiency of aptamer-*Bo*NT/A binding, the efficiency of folding of the aptamer itself, and the efficiency of immobilization of the aptamer on the surface. In the surface recognition process, both the binding of the aptamer to *Bo*NT/A and self-folding of the aptamer occur on the surface; the immobilization efficiency relates only to the aptamer itself. In the in-solution recognition process, both the binding of the aptamer to *Bo*NT/A and self-folding of the aptamer occur in solution. In contrast to the surface recognition process, in-solution immobilization efficiency relates to the aptamer-*Bo*NT/A complex. Figure 3 shows amperometric detection data for these two types of assay.

Figure 3 shows that the signal generated by recognition in solution is approximately 900 nA higher than that generated by recognition on the surface. The SNR is 6.8 for in-solution recognition and 1.3 for the surface recognition. Background levels are low in both processes (observed differences in background may be the result of the different buffers used in the immobilization and recognition processes). With the low surface concentration of streptavidin (0.30±0.05 pmol/cm^2), crowding effect is not the critical problem for aptamer surface binding. Since the concentrations of aptamer and *Bo*NT/A toxoid are identical in the two processes, the only difference is the medium in which recognition takes place. As discussed earlier, the SNR depends on the correct folding of the aptamer. Therefore, the aptamer in solution has higher binding and self-folding efficiency than the aptamer immobilized on the surface. One possible explanation for this phenomenon is that the aptamer in solution can fold freely and has a greater chance of interacting with target *Bo*NT/A toxoid in three dimensions, resulting in a higher possibility of correctly folding and docking with target. However, folding of the aptamer on the surface of the electrode may be constrained by chemical or physical interactions between the aptamer and the surface; docking with the target toxoid may be similarly restricted. Based on the assumption that attachment of the aptamer to the surface hinders the recognition of aptamer and target toxoid in this manner, the remaining experiments were carried out using recognition in solution.

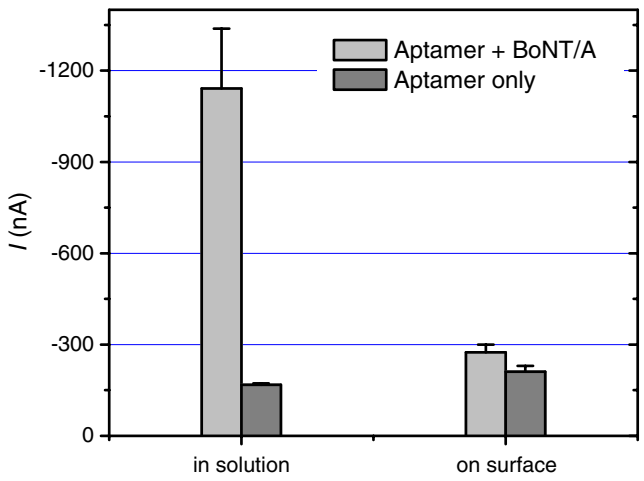

Fig. 3 Aptamer-based detection by recognition on the surface and in solution in the presence of 100 ng/ml *Bo*NT/A toxoid

Folding time and potassium concentration in aptamer-based *Bo*NT/A detection

Four different incubation times were investigated for aptamer folding in in-solution recognition.

Amperometric data in Table 1 show that 1 h of incubation results in poor recognition and an SNR of only 1.5. Both the sample and blank control had a current in the range −200 to −400 nA. As the incubation time increased, the signal for sample toxoid binding increased. After 24 h of incubation, the current of *Bo*NT/A reached −1986 nA, which is 5.3 times higher than that seen for the 1-h incubation. Meanwhile, as the sample signal increased between 1 h and 24 h of incubation, the background signal

Table 1 Amperometric detection of *Bo*NT/A toxoid following different incubation times

Incubation time (hours)	I_{sample}[a]/nA	I_{blank}[b]/nA	*SNR*
1	−376±64	−256±26	1.5
3	−1142±197	−168±5	6.8
5	−1204±100	−100±2	12.0
24	−1986±42	−52±6	38.2

[a] I_{sample} is the current measured at a *Bo*NT/A toxoid concentration of 100 ng/ml

[b] I_{blank} is the current measured in the absence of *Bo*NT/A toxoid

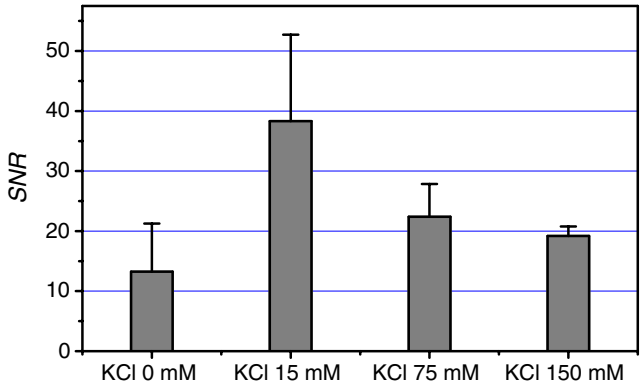

Fig. 4 Concentration profile for aptamer-based detection in the presence of 100 ng/ml *Bo*NT/A toxoid after 24 h of incubation in buffer containing 0, 15, 75, or 150 mM KCl

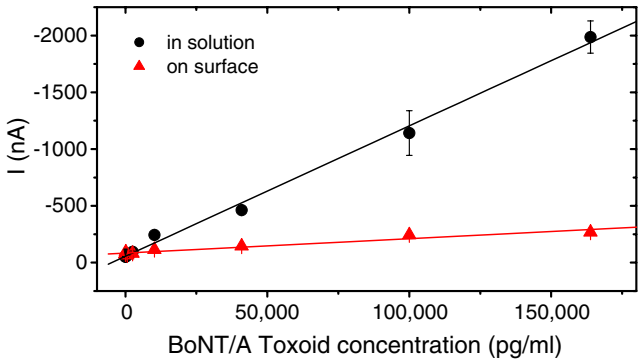

Fig. 5 Concentration profile for aptamer-based detection of *Bo*NT/A toxoid after 24 h of incubation in solution and on surface with buffer containing 15 mM KCl. Linear regression constant for recognition in solution is R^2=0.99, and for recognition on surface the results is R^2= 0.94. The LOD is 40 pg/ml for recognition in solution and 2,560 pg/ml for recognition on surface, with criteria of two standard deviations above the blank control

decreased from −256 nA to −52 nA and, following 24 h of incubation, the SNR was 38. In the remainder of the experiments, an incubation period of 24 h was used.

Another important parameter for aptamer folding and binding to *Bo*NT/A is the concentration of metal ions in the solution [27–30]. Metal cations have been observed to either stabilize or induce conformational change in aptamers [31]. Metal cations also play an important role in *Bo*NT folding [32]. Among the alkali and earth alkali metals commonly observed in biological systems, the potassium ion has a diameter that fits well in the cavities between guanine tetrads and potassium ion concentration is highly correlated with the folding and docking of aptamers [23]. Therefore, four reaction buffers containing different concentrations of potassium ion were investigated (Fig. 4). The correlation between potassium ion concentration and signal intensity was not simply linear. An optimal potassium ion concentration of 15 mM was associated with the highest signal and lowest background. Concentrations of 0, 75, and 150 mM were associated with low signal and high background.

The concentration profile for *Bo*NT/A-aptamer binding was obtained under the optimized assay conditions of 15 mM KCl and 24 h of incubation in solution (Fig. 5). With the criterion of cutoff at two standard deviations (SDV), the dynamic range extended from 100 ng/ml to 40 pg/ml and the limit of detection (LOD) was 40 pg/ml. The optimized LOD of the aptamer-based electrochemical sensor is comparable to that of the conventional immunoassay for *Bo*NT detection (LOD 2–60 pg/ml) [6]. The concentration profile with surface recognition was also listed for comparison with the LOD of 2,560 pg/ml. The surface recognition process between *Bo*NT/A and *Bo*NT/A aptamer on surface shows a Langmuir model with the binding constant $K=2.0\pm0.5\times10^{-6}$ $(\text{pg/ml})^{-1}$ $(3.0\pm0.8\times10^{9}\ \text{M}^{-1})$. This binding constant is relatively lower than the $1/K_d$s $(3.3\times10^{8}\ \text{M}^{-1})$ from Tok's work [11], which was done on microbeads in solution. The lower K of *Bo*NT/A provides the supporting evidence that the binding efficiency on flat gold surface is lower than that in solution. In addition, the signal is not saturated with concentration below 150 ng/ml *Bo*NT/A. Therefore, the crowding effect is not the major reason for the low SNR from surface recognition process. The primary advantage of the aptamer-based approach is that it precludes the necessity of generating a specific monoclonal antibody and much shorter and simpler procedure compared with immunoassay.

Discussion

Here, we report an aptamer-based *Bo*NT/A detection system that displays specific signal amplification and a high SNR and is based on conformational change in the aptamer induced by steric hindrance. This steric hindrance is caused by either the opened or closed conformation of the aptamer [17, 33]. When the aptamer binds to target *Bo*NT/A toxoid it is in its open state and signal increases. If the target is not bound, the aptamer remains in its closed conformation, resulting in low signal. Unlike a traditional hairpin probe, which is designed with an inner stem region so it can be triggered to open or close, this specific *Bo*NT/A aptamer does not contain such a "switch" in the sequence. However, this aptamer has a relatively long sequence of 76 bp and two interior G-quadruplexes. Therefore, the aptamer will be in a tightly coiled, or closed, state in the absence of *Bo*NT; after binding to *Bo*NT conformational change occurs. Most aptamer–protein binding events consist of multi-point docking or surface–surface interactions, rather than simple point–point docking. This complex

docking process results in the open conformation of the *Bo*NT/A aptamer.

In our optimization of incubation time, we observed that short incubation times resulted in very low SNRs, while longer incubation times resulted in high SNRs. One possible explanation for this observation is based on the reaction energy. A high energy barrier would exist and several misfoldings would occur during the reaction process, resulting in different quasi-stable intermediates. Although the appropriate configuration is the most stable one and has the lowest Gibbs free energy, trapping in the quasi-stable intermediates can occur. In our investigation, short durations of folding (less than 3 h of incubation) generated an SNR of only 1.5, while longer-duration (greater than 5 h) incubations generated SNRs of 12 or greater (SNR of 38 after 24 h of incubation). This data provides evidence supporting the existence of quasi-stable, misfolded conformational intermediates prior to achievement of the final stable conformation.

To drive the reaction toward the thermodynamically stable product, an important factor for correct folding is the ion composition of the reaction buffer. Our data show that the affinity of the aptamer for *Bo*NT/A is dependent on the potassium ion composition of the buffer, with a concentration of 15 mM KCl generating the highest SNR. With the potassium concentration optimized, the aptamer binds to *Bo*NT/A with high affinity and the LOD of the sensor is 40 pg/mL (400 fM). Other metal ions in addition to K^+ should also affect the folding of aptamer, including Ca^{2+}, Mg^{2+}, Na^+. Meanwhile, the folding process is also influenced by more than a single type of ion and future work will investigate optimized concentrations of combinations of multiple types of ions, such as sodium, potassium, magnesium, and calcium.

Conclusion

Steric hindrance resulting from the structure of the aptamer introduces specific and high signal after the aptamer binds to *Bo*NT/A toxoid. The binding affinity of the aptamer for *Bo*NT/A toxoid depends on correct folding of the aptamer. Optimized incubation time and potassium ion concentration results in a high signal-to-noise ratio. The LOD is 40 pg/ml under optimized conditions within 24 h, which is much shorter than the current record, 4 days.

Acknowledgments This work was supported by funds from the NASA National Space Biomedical Research Institute (TD00406), the Pacific-Southwest Center for Biodefense and Emerging Infectious Diseases Research UC Irvine/NIH NIAID Award (1 U54 AI 065359) 2005–1609, National Institutes of Health/National Institute of Dental and Craniofacial Research (UO1DE 017790, UO1DE015018, and RO1DE017593) and the National Institutes of Health Nanomedicine Roadmap (Center for Cell Control, PN2EY018228).

References

1. Kostrzewa RM, Segura-Aguilar J (2007) Neurotox Res 12:275–290
2. Simpson LL (2004) Annu Rev Pharmacol Toxicol 44:167–193
3. Wein LM, Liu YF (2005) Proc Natl Acad Sci USA 102:9984–9989
4. Arnon SS, Schechter R, Inglesby TV, Henderson DA, Bartlett JG, Ascher MS, Eitzen E, Fine AD, Hauer J, Layton M, Lillibridge S, Osterholm MT, O'Toole T, Parker G, Perl TM, Russell PK, Swerdlow DL, Tonat K (2001) JAMA J Am Med Assoc 285:1059–1070
5. Stanker LH, Merrill P, Scotcher MC, Cheng LW (2008) J Immunol Methods 336:1–8
6. Sharma SK, Ferreira JL, Eblen BS, Whiting RC (2006) Appl Environ Microbiol 72:1231–1238
7. Attree O, Guglielmo-Viret V, Gros V, Thullier P (2007) J Immunol Methods 325:78–87
8. Liao W, Randall BA, Alba NA, Cui XT (2008) Analytical and Bioanalytical Chemistry 392:861–864
9. Song SP, Wang LH, Li J, Zhao JL, Fan CH (2008) Trac Trends Anal Chem 27:108–117
10. Liao W, Cui XT (2007) Biosens Bioelectron 23:218–224
11. Tok JBH, Fischer NO (2008) Chem Commun 1883–1885
12. Xiao Y, Lai RY, Plaxco KW (2007) Nature Protocols 2:2875–2880
13. Lai RY, Plaxco KW, Heeger AJ (2007) Anal Chem 79:229–233
14. de-los-Santos-Alvarez N, Lobo-Castanon MJ, Miranda-Ordieres AJ, Tunon-Blanco P (2008) Trac Trends Anal Chem 27:437–446
15. Wei F, Sun B, Guo Y, Zhao XS (2003) Biosens Bioelectron 18:1157–1163
16. Huang TJ, Liu MS, Knight LD, Grody WW, Miller JF, Ho CM (2002) Nucleic Acids Res 30:e55
17. Wei F, Wang JH, Liao W, Zimmermann BG, Wong DT, Ho CM (2008) Nucleic Acids Res 36:e65
18. SantaLucia J (1998) Proc Natl Acad Sci USA 95:1460–1465
19. Zuker M (2003) Nucleic Acids Res 31:3406–3415
20. Kikin O, D'Antonio L, Bagga PS (2006) Nucleic Acids Res 34: W676–W682
21. Schuhmann W, Kranz C, Wohlschlager H, Strohmeier J (1997) Biosens Bioelectron 12:1157–1167
22. Gau V, Ma SC, Wang H, Tsukuda J, Kibler J, Haake DA (2005) Methods 37:73–83
23. Shim J, Tan Q, Gu L (2008) Nucleic Acids Res doi:10.1093/nar/gkn968.
24. Schultze P, Hud NV, Smith FW, Feigon J (1999) Nucleic Acids Res 27:3018–3028
25. Wei F, Qu P, Zhai L, Chen CL, Wang HF, Zhao XS (2006) Langmuir 22:6280–6285
26. Chen CL, Wang WJ, Wang Z, Wei F, Zhao XS (2007) Nucleic Acids Res 35:2875–2884
27. Brion P, Westhof E (1997) Annu Rev Biophys Biomol Struct 26:113–137
28. Juskowiak B (2006) Anal Chim Acta 568:171–180
29. Draper DE (1996) Trends Biochem Sci 21:145–149
30. Ruta J, Ravelet C, Desire J, Decout JL, Peyrin E (2008) Analytical and Bioanalytical Chemistry 390:1051–1057
31. Noeske J, Schwalbe H, Wohnert J (2007) Nucleic Acids Res 35:5262–5273
32. Encinar JA, Fernandez A, Ferragut JA, Gonzalez-Ros JM, DasGupta BR, Montal M, Ferrer-Montiel A (1998) Febs Lett 429:78–82
33. Wei F, Chen CL, Zhai L, Zhang N, Zhao XS (2005) J Am Chem Soc 127:5306–5307